Awashra, Mohammad; Elomaa, Pinja; Ojalehto, Tuomas; Saavalainen, Päivi; Jokinen, Ville

Superhydrophilic/Superhydrophobic Droplet Microarrays of Low Surface Tension Biofluids for Nucleic Acid Detection

Published in:
Advanced Materials Interfaces

DOI:
10.1002/admi.202300596

Published: 04/01/2024

Document Version
Publisher's PDF, also known as Version of record

ADVANCED MATERIALS INTERFACES
Open Access
www.advmatinterfaces.de

Superhydrophilic/Superhydrophobic Droplet Microarrays of Low Surface Tension Biofluids for Nucleic Acid Detection

Mohammad Awashra, Pinja Elomaa, Tuomas Ojalehto, Päivi Saavalainen, and Ville Jokinen**

Superhydrophilic/superhydrophobic patterned surfaces can be used to create droplet microarrays. A specific challenge with the liquids needed for various biomedical applications, as compared to pure water, is their lower surface tension and potential for contaminating the surfaces through adsorption. Here, a method is shown to create biofluid droplet microarrays using discontinuous dewetting of pure water, an oil protective layer, and finally biofluid exchange with the water droplet array. With this method, a droplet array of a viscous nucleic acid amplification solution can be formed with a low surface tension of 34 mN m^{-1} and a contact angle of only 76° with the used hydrophobic coating. This droplet array is applied for nucleic acid detection of SARS-CoV-2 virus using strand invasion-based amplification (SIBA) technology. It is shown that by using an array of 10 000 droplets of 50 µm diameter the limit of detection is 1 RNA copy μL^{-1}. The results demonstrate that SIBA on droplet microarrays may be a quantitative technology.

1. Introduction

Sample partitioning to tiny droplets is required to perform many bioassays such as digital nucleic acid detection. There are mainly three approaches to partitioning aliquots into droplets of controlled volume. First, droplet microfluidics, where a microfluidic pump is used to serially generate water droplets confined in a second immiscible continuous phase. The drawbacks of this method are its requirement for constant flow and proper surfactants, and the possibility of droplets destabilization during processing, resulting in cross-contamination and droplets merging. Second, solid microchambers/wells, where the droplets are confined in a solid container. This method does not need surfactants and unlike microfluidics droplets, the formed droplets have a defined location, enabling simple indexing of each droplet. The solid walls prevent droplet merging and cross-contamination and enable a very uniform volume distribution of the droplets.[1] Third, 2D open droplet microarray (also called surface droplets) where the droplets are loaded on a flat surface by a printing method,[2–4] or by discontinuous dewetting using a patterned surface with selective hydrophilic/hydrophobic modification.[5] While microwells and water-in-oil droplets are frequently used for sample partitioning, surface droplet microarrays can be considered a combination of both, where there is a microarray of accessible droplets (as in water-in-oil droplets), and at the same time, the droplets are fixed in position and more controllable (as in microwells). Moreover, instead of the oil phase or physical wall separation, the droplets can be separated using a patterned superhydrophobic barrier.[1,6–8]

Nucleic acid testing is extensively applied in biomedical fields. The detection of pathogens, such as SARS-CoV-2, is normally realized by nucleic acid amplification. Reverse transcription-quantitative polymer chain reaction (RT-qPCR) is currently the gold standard for nucleic acid detection.[9,10] However, RT-qPCR assays are based on relative quantification, which necessitates an external calibration using genetic standards or internal reference DNA templates.[11] On the other hand, digital PCR (dPCR) relies solely on the count of positive partitions rendering the standard curve requirement unnecessary. Consequently, dPCR achieves superior sensitivity and accuracy in comparison to qPCR.[3] One of the requirements of dPCR is the partition of the diluted nucleic acid sample into a huge number of separate microreactors.[12,13] Performing dPCR in commercial equipment is significantly more expensive than conventional PCR.[14] Developing a point of care (POC) device that makes dPCR not only more sensitive but also cheaper, is a crucial matter. Microstructured devices are used

M. Awashra, V. Jokinen
Department of Chemistry and Materials Science
School of Chemical Engineering
Aalto University
Tietotie 3, Espoo 02150, Finland
E-mail: mohammad.awashra@aalto.fi; ville.p.jokinen@aalto.fi
P. Elomaa, P. Saavalainen
Translational Immunology Research Program
Folkhälsan Research Center
University of Helsinki
Haartmaninkatu 8, Helsinki 00290, Finland
T. Ojalehto
Aidian Oy
Koivu-Mankkaan tie 6 B, Espoo 02200, Finland

The ORCID identification number(s) for the author(s) of this article can be found under https://doi.org/10.1002/admi.202300596

DOI: 10.1002/admi.202300596

for dPCR and integrated into POC devices.[15] Several studies used water-in-oil droplet microfluidics for dPCR analysis.[16] Others reported the use of solid microchambers/wells.[17–25] While these methods make it hard to access the droplet and can have complex droplet loading methods, surface microarrays make the droplet very accessible and addressable. This approach simplifies the manipulation of droplets, enabling direct analysis on the chip using various optical and other techniques.[1] When the PCR solution gets partitioned into a droplet microarray, following Poisson distribution, most of the droplets theoretically will contain only one or zero target molecules.[13] Each copy is then individually amplified by PCR.

The amplification techniques of nucleic acid fall into one of the two categories: thermocycling amplification or isothermal amplification.[15] The thermocycling technique requires complex and time-consuming rapid temperature changes during amplification. In contrast, isothermal amplification is a one-step heating process, making it simpler and implementable in portable and POC devices. Isothermal amplification systems include nucleic acid sequence-based amplification (NASBA), loop-mediated isothermal amplification (LAMP), and many other reactions.[15] Another isothermal amplification technique is Strand Invasion Based Amplification (SIBA) that was first described in 2014.[26] SIBA works at relatively low temperatures, which lowers the evaporation rate of tiny droplets. SIBA takes advantage of target template denaturation that is mediated by recombinase enzyme and invasion oligonucleotide (IO). Local disruption of double-stranded DNA (dsDNA) is created to target the template allowing amplification primers to anneal. A single-stranded binding protein stabilizes the dsDNA and prevents re-annealing between the two separated DNA stands. Due to the enzymatic denaturation step, amplification can be carried out at a constant temperature (≈44 °C). Target-specific IO has 3′ end 2′-O-methyl RNA modification that prevents it from acting as a template for the polymerase. This makes SIBA highly specific and resistant to any non-specific amplification, enabling high sensitivity for a single target molecule.[26,27]

In this study, a facile droplet microarray was developed to spatially separate aliquots of a controlled volume of SIBA reaction mixture. The array consists of circular superhydrophilic (SHL) patterns of varying size (50–500 µm) separated by superhydrophobic (SHB) black silicon barriers. The reagent loading method was optimized to solve complications arising from the adsorption and surface tension of the SIBA mixture. The SIBA mixture was successfully partitioned into droplet microarray using the developed protective oil method. The low temperature used in isothermal SIBA technology (44 °C for 20 min) is a clear advantage for dPCR experiments where such exceedingly small droplet volumes are used. We show the detection and quantification of SARS-CoV-2 RNA down to 1 copy μL^{-1}.

2. Results and Discussion

2.1. SHL/SHB Black Silicon Surface Characterization

The black silicon (bSi) nanograss structure is shown in **Figure 1**a. The bSi surface was patterned into superhydrophilic circular spots with superhydrophobic borders using a fluoropolymer coating. This process was used to fabricate 40 different combinations of SHL spot sizes and spacings. The interface of the coated and oxidized bSi and their static contact angles (CAs) are shown in Figure 1b. Water droplet microarray (DMA) spontaneously formed on the patterned bSi by discontinuous dewetting. The nanograss structure increases the solid area for the Wenzel state on the SHL spot and minimizes it for the Cassie state on the SHB regions (nano tips) making an extreme wettability difference between the two regions. Figure 1c shows the trapped air plastron (silver-like color) beneath the water film indicating a Cassie wetting state, while the SHL spots appear in black indicating full wetting of the surface (Wenzel state). Figure 1d,e shows top and side views of the water DMA, respectively.

To understand the DMA formation and select the optimal parameters for carrying out quantitative nucleic acid detection, different SHL spot sizes and spacings were fabricated (see Table S1, Supporting Information). The aim was to fit in as many spots as possible without merging nearby droplets. Droplet formation and evaporation in ambient air were monitored for chips with SHL spot sizes of 50–500 µm with different spacings under optical microscopy (Figure S1, Supporting Information). Droplet evaporation on different chips was studied in ambient air at room temperature (21 °C) and room relative humidity (40%) (Figure 1f). The evaporation time of the DMA was found to increase with SHL spot size and decrease with spacing for all the combinations of spot sizes and spacings (Figure S2a, Supporting Information). The larger droplets have a higher volume-to-surface ratio, and therefore, slower evaporation rate. With increasing droplet density, the atmospheric surrounding of the droplets is more saturated in water vapor, which also slows down the evaporation rate.

The volume of the water droplet for the different arrays was measured using goniometry. The volume distribution of the droplets in an array is narrow, making the array suitable for applications that require uniform droplet volumes. The droplet volume is increasing from 0.1–10 nL with spot diameter at fixed 50 µm spacing (Figure 1g). This increase is exponential as a cube of spot diameter [$V\,(nL) = 10^{-7}\,d^{2.92}(\mu m)$, $R^2 = 0.997$] following the behavior of semi-spherical water droplets, which is also confirmed by other studies.[6,28,29] Xu et al.[28] obtained the equation $V\,(nL) = 32.9d^{2.44}(mm)$, which is more deviated than our results compared to the spherical droplet volume (d^3). However, the range of the spot diameter they used was 0.3–2 mm making the effect of the gravity a major factor in determining the shape of the droplet, while we used 50–500 µm spots that are small enough to avoid high gravitational forces. Moreover, this group used the beads counting method to measure droplet volume while in our case goniometry was used. The droplet volume also increased from 5.4–8.9 nL as the spacing between the 400 µm sized spots increased from 50–800 µm (Figure 1g). A study by Chang et al.[30] showed that the droplet volume of hydrophilic squared spots with a diameter of 500 µm and different spacing of 0.2–0.5 mm gives a droplet volume of ≈12–14 nL, which is in perfect agreement with our values for this spot size (10–12 nL, see Figure S2b, Supporting Information). The droplet evaporation rate for the array with larger spacing is faster, even though the droplet volume is bigger, indicating that the vapor saturation factor had the advantage over the small increase of droplet volume. According to Mandsberg et al.[29] The volume of the droplets can be affected by the withdrawing velocity and angle of the chips from the water. The

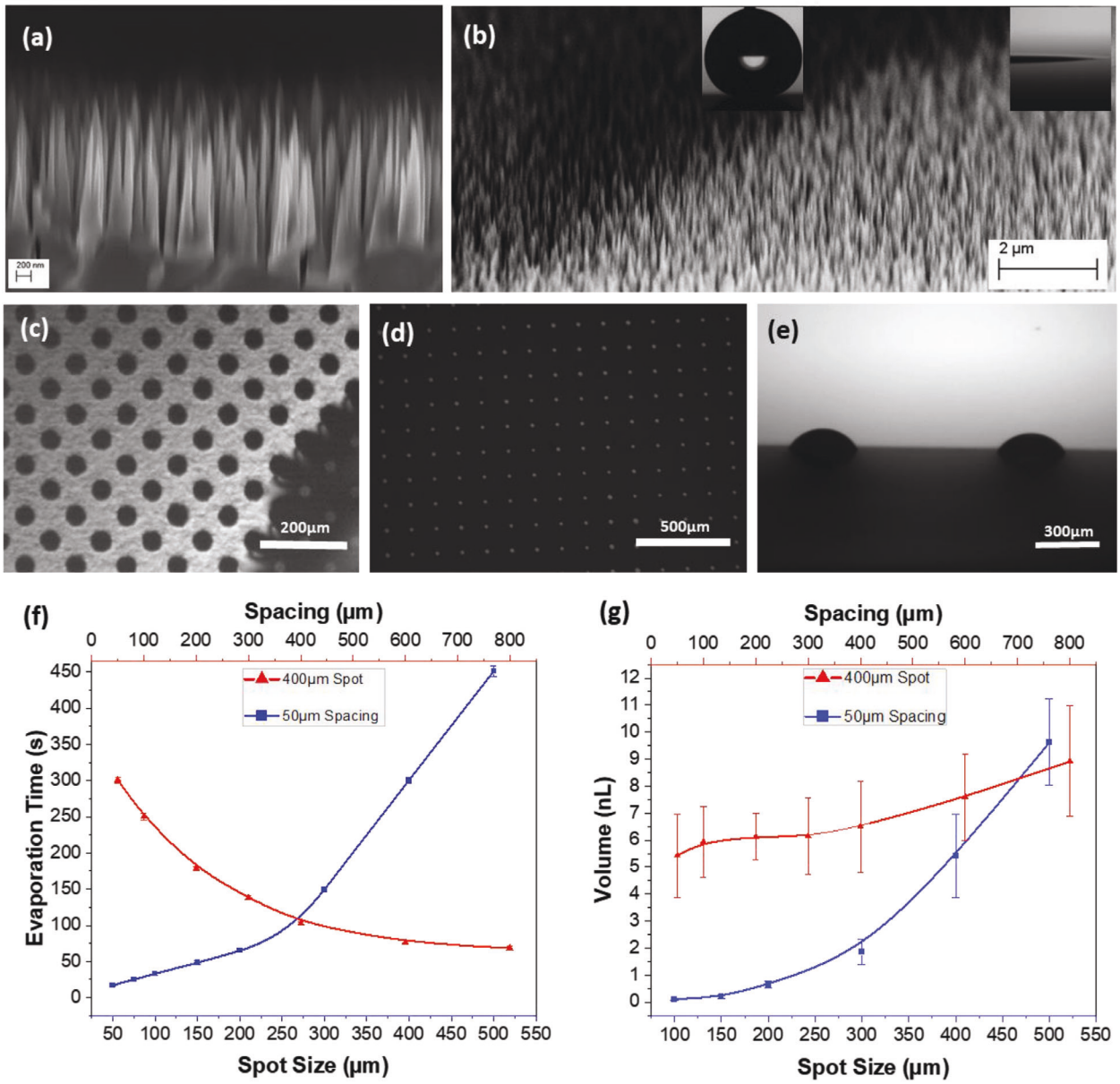

Figure 1. Water droplet array formation on SHL/SHB bSi surface. a) Scanning electron microscopy (SEM) image of the nanograss structure of bSi. b) SEM image of the interface between the fluoropolymer-coated SHB (left) and the oxidized non-coated SHL (right) bSi nanograss and corresponding contact angles. c) bSi chip immersed in water. A water film covers the surface and fully wets the SHL spots (black circles) while the SHB regions have a Cassie wetting state with air plastron (silver-like color). d,e) Top and side views of the water droplet microarray, respectively. The effect of SHL spot size (blue square) and spacing (red triangle) on the water droplet f) evaporation time and g) volume.

withdrawal of the chip in this study was done manually but we kept a fixed protocol using the maximum possible velocity and an angle in the range of 10 –30°. It is worthy to mention here that the camera resolution of the goniometer did not allow an accurate volume measurement of droplets on smaller spot sizes like 50 µm.

The array chip measuring 50 × 50 µm in size and spacing was selected for subsequent experiments. The spot size 50 µm allows an easy formation of the droplets besides having the highest droplet density with this size. While the spacing 50 µm is optimal for this size since it gives the highest possible droplet density without having any droplets merging or film formation. The droplet density of this array is 10 000 droplets cm^{-2}.

2.2. Wettability and Surface Tension Characterization

Unlike pure water, the SIBA reaction mixture did not form discrete droplets spontaneously by simply immersing the array in the liquid. This complication is shown in **Figure 2**a that shows that there is no plastron (no Cassie state) when this mixture is

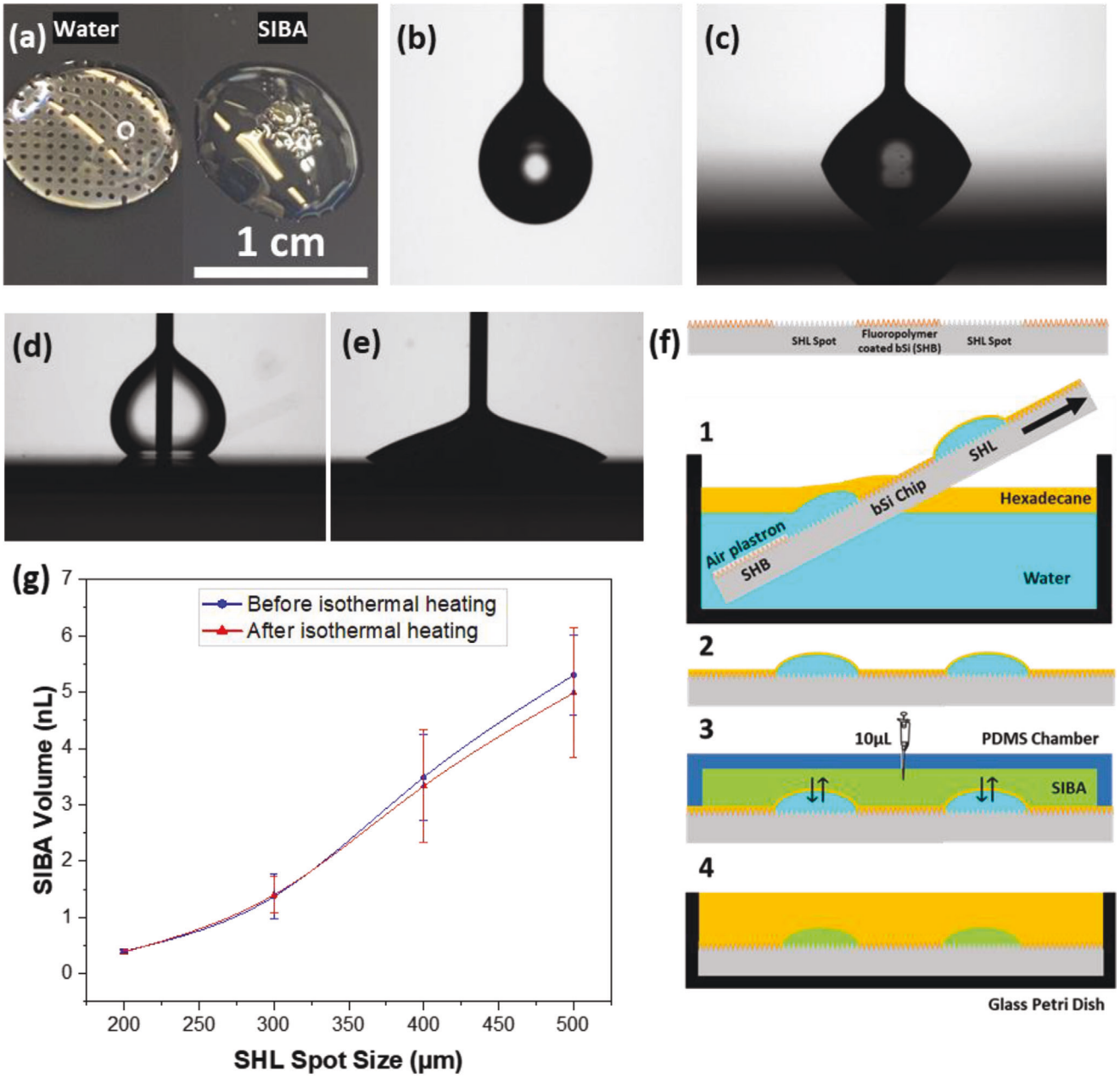

Figure 2. Wettability characterization for developing a reliable method for creating droplet microarrays out of SIBA reaction mixture. a) While water (left) has two different wettability states on the SHL and SHB regions of the bSi surface, the SIBA mixture (right) has the same wettability state on both, preventing the formation of MDA. b) Surface tension measurement of SIBA (34 mN m^{-1}) using pendant droplet method. c) The advancing contact angle of SIBA mixture on the HB surface in the air (76°). The advancing contact angle of SIBA under hexadecane on d) HB surface (149°) and e) HL surface (31°). The needle diameter in (b–e) is 0.25 mm. f) The workflow of the SIBA mixture DMA formation. g) SIBA droplet volume of different SHL spot sizes (spacing is fixed at 50 µm) before (blue) and after (red) isothermal heating at 44 °C for 20 min.

used. The key differences between the two liquids can be: the surface tension, the viscosity, and the potential of molecule adsorption from the SIBA reaction mixture. Ramalingam et al.[31] claimed that the fluid properties of PCR solution are different from that of pure water, where they found that Promega PCR static CA on polydimethylsiloxane (PDMS) surface is 46° (as compared to water that has a roughly 100° static CA with PDMS) and its surface tension is ≈31 mN m^{-1} (72 mN m^{-1} for water). Some other studies that used PCR solution often approximate its properties to that of pure water.[31]

Therefore, to develop a method for the reliable formation of droplet arrays of PCR solutions, we characterized the surface tensions and wetting properties of water, the nucleic acid amplification solution (SIBA mixture), and hexadecane oil on two types of surfaces. First, the surface tension of the SIBA mixture was measured using the pendant droplet method and found to

Table 1. Advancing and receding contact angles of a system formed of water, SIBA, and hexadecane on HL and HB surfaces.

Experiment	Adv. CA [°]	SD [°]	Rec. CA [°]	SD [°]
Water droplet in air vs HL	20	0,5	0*	-
Water droplet in air vs HB	114	0,2	97	0,2
Hexadecane droplet in air vs HL	0	-	0	-
Hexadecane droplet in air vs HB	50	0,5	36	0,5
SIBA droplet in air vs HL	8	0,8	0	-
SIBA droplet in air vs HB	76	1	0	-
Hexadecane droplet under SIBA vs HB	180	-	-	-
Hexadecane droplet under SIBA vs HL	180	-	-	-
Hexadecane droplet under water vs HB	70	1	36	0,5
Hexadecane droplet under water vs HL	167	5	161	2,5
SIBA droplet under hexadecane vs HB	149	1	0	-
SIBA droplet under hexadecane vs HL	31	0,8	0	-

HL: hydrophilic; **HB**: hydrophobic; **Adv. CA**: advancing contact angle; **Rec. CA**: receding contact angle; **SD**: standard deviation; **SIBA**: strand invasion-based isothermal amplification technology for nucleic acid detection. *Any contact angle lower than 5° (what the goniometer can measure) was recorded as 0°.

be 34 mN m^{-1} (±0.2 mN m^{-1}) (Figure 2b). While pure water and pure hexadecane surface tensions were found to be 72 and 27 mN m^{-1}, respectively. The contact angle measurements were performed with planar silicon surfaces which have the same two surface chemistries as we use on the bSi arrays. The reason for utilizing planar surfaces is that we were interested in the thermodynamic question of whether liquid **A** can replace liquid **B** on a given surface. This depends only on the chemistry and not on the topography. **Table 1** summarizes the CA measurement results. First, the advancing (adv.) and receding (rec.) CAs for water, SIBA, and hexadecane were measured on both surfaces in ambient air. Focusing on the hydrophobic (HB) surface, the adv. CA of water, SIBA, and hexadecane were 114°, 76°, and 50°, respectively. Water is clearly having a non-wetting behavior on the fluoropolymer-coated HB surface. Alternatively, SIBA and hexadecane have a wetting behavior (CA <90°). The lower CA of SIBA (Figure 2c) can be explained by its lower surface tension ($cos(\theta) = \frac{\gamma_{sv} - \gamma_{sl}}{\gamma_{lv}}$).

For water, as the CAs are > 90° on the HB surface and < 90° on the HL one, this leads to the possibility of spontaneous discrete droplet formation (i.e., by discontinuous dewetting) on the bSi array (in fact this happened with all spot sizes and spacings we tested). In contrast, for the SIBA mixture, both the HL and HB surfaces have CAs that are < 90°, which means that there is no possibility for discrete droplet formation since the Cassie state is not obtained on the bSi samples and the Wenzel state only enhances the wetting further. As a result of that, we observed the formation of a stable continuous film over SHL and SHB regions on the bSi surface without spontaneously splitting into droplets.

To complicate further, the rec. CA of SIBA on both HL and HB surfaces was 0° indicating strong adhesive forces with both surfaces. This has led to SIBA not receding from both SHL and SHB regions of the bSi surface confirming that SIBA droplet array formation is non-spontaneous. However, SIBA wettability was also investigated under hexadecane, and it was found that SIBA cannot replace hexadecane on the HB surface (adv. CA > 90°, Figure 2d), nonetheless, on the HL surface, it can (adv. CA < 90°, Figure 2e).

To make the SIBA mixture array formation more reliable, we developed the protective oil method shown in Figure 2f. First, (**1** and **2**) a water droplet microarray is formed on the SHL/SHB pattern and then covered with a thin layer of hexadecane. Next, (**3** and **4**) the SIBA mixture was added on top with the assistance of a PDMS chamber and was kept for 5 s, which was found to be sufficient exchange time but was not optimized downward further. The key idea of this method is applying the protective oil coating on the SHB region to prevent the adsorption of the biofluid contents while, at the same time, protecting the SHL spots using water. As shown by the CA measurements, the biofluid can replace water from the SHL spots, but it cannot replace oil in the SHB region. We assume that the exchange process between SIBA and water is most probably a hydrodynamic process where the thin oil layer on top of the protruding water droplets gets sheared away so that the SIBA droplet makes direct contact with the chip forming SIBA droplet. The SIBA droplet microarray was successfully formed and can be seen by the naked eye if 200 µm spots are used as shown in Figure S3 (Supporting Information). The isothermal SIBA amplification is performed at 44 °C for 20 min, and therefore, possible evaporation of the droplets under these conditions was studied. Figure 2g shows that the droplet's volume remained nearly unchanged before and after undergoing the heating step while the droplets were covered with hexadecane oil.

For the validation of our method, two other biofluids were applied on the chip using the steps in Figure 2f. First, Evagreen dye with high concentration of DNA solution was used to confirm the exchange process between the biofluid and water droplets. The results indicated high fluorescence for the imaged droplets as shown in Figure S4a (Supporting Information). Second, a non-fluorescent protein-rich cell media was used to form the droplet microarrays. The microarray was successfully formed as shown in Figure S4b (Supporting Information). As droplet microarrays were formed on our chip for three biofluids, we concluded that the protective oil method could be used to overcome the challenges caused by the different properties of biofluids.

Patterned SHL/SHB surfaces have been employed to perform different bioassays. Our previous study used SHL/SHB bSi array for single-cell trapping by splitting cell media into tiny droplets.[8] Popova et al.[6] used a SHL/SHB droplet microarray for high-throughput cell-based screening. Qian et al.[32] formed 10^6 femtoliter droplets array using a patterned perfluorinated surface to perform bead-free digital immunoassay for human interleukin-6. Nevertheless, some bioassays employ biofluids with properties that differ greatly from water, especially surface tension, viscosity, and adsorption capabilities.[33] Peethan et al.[34] studied the effect of surface tension of a CTAB (cetyl trimethyl ammonium bromide) solution on droplet splitting to a droplet microarray on a candle-soot-coated patterned SHL/SHB surface. The surface tension of the solution varied from 61 to 38.5 mN m^{-1} with varying concentrations of CTAB, and the authors found that the droplet is still splitting into arrays and the daughter droplet volume remains nearly the same. They concluded that the substrate can be used for making bioassays using body fluids like blood. However, surface tension is not the only factor that can affect the splitting behavior of the droplets. Protein and other biomolecules can get

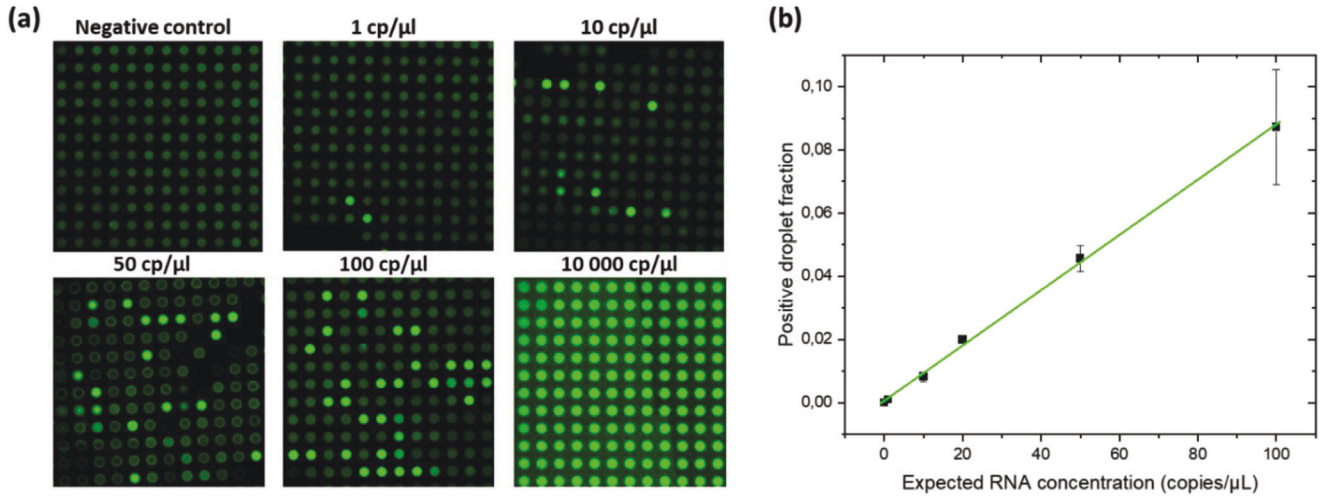

Figure 3. a) Fluorescent images of the dSIBA quantification experiment performed with SARS-CoV-2 RNA concentrations ranging from 0 to 10 000 copies μL^{-1} using SHL/SHB bSi droplet microarray platform. b) Shows a strong linear correlation between the counted positive droplets and expected RNA concentration. 10 000 cp μL^{-1} is not included in the curve.

adsorbed and contaminate the surface changing its wettability. We noticed this effect by the rec. CA of 0° of SIBA mixture on our surface indicating strong adhesion and Wenzel state. Wang et al.[35] showed that bovine serum albumin (BSA) protein solution causes loss in air plastron of an SHB surface as soon as they are immersed in the protein solution, indicating a Cassie to Wenzel state transition. They attributed this behavior to two factors: the lower surface tension of the BSA solution (≈50 mN m^{-1}), and the protein adsorption on the SHB substrate.

2.3. Digital SIBA – Isothermal Amplification on the Droplet Microarray

In this study, SARS-CoV-2 SIBA assay is used to test the performance of the designed SHL/SHB bSi 2D- open droplet microarray platform. SIBA is an isothermal amplification technology for nucleic acid testing[26] that works at low temperatures (44 °C). It has been used before in a droplet microfluidics system (Elomaa et al 2023, unpublished). Hexadecane oil was not found to affect the SIBA amplification based on the real-time amplification experiment conducted using RT-qPCR machine.

Before the use of the patterned chips for digital SIBA (dSIBA) reaction, they were sterilized using a UV lamp. The sterilization was found to not affect the hydrophobic coating and the wettability of the chip. Several fabricated arrays with different spot sizes and spacings were used to perform dSIBA, and the depicted results showed a successful formation of SIBA droplet array using our method (Figure 2f), and the fluorescent positive droplets were imaged and are shown in Figure S5 (Supporting Information). The 50 × 50 µm chip was used to perform a quantification test of dSIBA assay. The quantification experiment was performed using a serial dilution of the target RNA and for negative control, a sample buffer was added without any target RNA. By partitioning the SIBA mixture into droplets on the platform, the dissolved target RNA copies are getting separately trapped in one of the 10 000 droplets formed on the 1 × 1 cm chip following Poisson statistics, which means that with low concentrations the spots contain only one or zero target.[17] Isothermal amplification of SIBA was performed at 44 °C for 20 min to amplify each trapped RNA copy in its droplet. The prepared concentrations were 1, 10, 20, 50, 100, and 10 000 copies μL^{-1}. The quantification results and a representative section of each experiment are shown in **Figure 3**. The differentiation between droplets lacking the target (negatives) and those containing it (positives) was accomplished by implementing a fluorescence amplitude threshold. The number of positive spots is clearly increasing with RNA concentration and the negative control has no signal (Figure 3a). Moreover, Figure 3b shows a strong linear relationship, with a correlation factor of 0.9986, between the expected target RNA concentration and measured positive spot fraction. This correlation indicates that dSIBA could be quantitative.[13,36]

We tested analyzing the positive and negative spots with Aiforia AI in addition to ImageJ thresholding. The results of both methods were very similar (See Figure S6, Supporting Information). One advantage of the surface array method is that it is very easy to analyze for several reasons: 1) The hydrophobic background is systematically completely black, 2) The spots are circles with a known diameter, and 3) The spots are in a known array. Because of these features, we concluded that the simpler ImageJ analysis was sufficient and reliable for our assay.

There is a trade-off in choosing a certain droplet size for the assay. The 50 × 50 µm chip that was characterized has a high density of droplets enabling it to detect high concentrations up to 10 000 copies μL^{-1} if 1 × 1 cm chip is used (Figure 3a), and its limit of detection is limited by the small total volume of the partitioned sample (1 copy μL^{-1}). Moreover, this spot size has the highest droplet density at which the droplet evaporation and image acquisition are well handled. At lower spot size like 25 µm the evaporation is extremely fast even under oil and the droplet cannot survive the isothermal heating step. On the other hand, arrays with much larger spots would have lower droplet density but higher single droplet volume. This would lead to worse quantification at higher concentrations due to a higher likelihood of

having multiple target RNA copies in a single spot. However, the total volume would be larger that would enable a lower limit of detection.

There are two previous studies that used SHL/SHB arrays for performing digital nucleic acid detection, both with a different nucleic acid amplification mixture. Chi et al.[37] fabricated hydrophilic/superhydrophobic pseudopaper photonic nitrocellulose substrate to perform digital LAMP (dLAMP). They used a spot diameter of 500 µm limiting their droplet array density. Mao et al.[38] used a polymethyl methacrylate (PMMA)-based SHL/SHB microfluidic chip to perform dLAMP. These groups did not clarify how they overcame the lower surface tension and adsorption complication of the LAMP mixture, compared to water. A major advantage of our method is that due to the protective hexadecane, the contents and properties of the biofluid should not matter as long as they cannot replace hexadecane (or other oil) from the SHB regions. This could enable the use of the same method for many types of biomedical droplet array applications.

3. Conclusion

We have reported in this study a superhydrophilic/superhydr ophobic patterned surface that can form a droplet microarray of a biofluid with different surface tension and molecular content compared to water. By applying a protective coating (hexadecane oil) to the superhydrophobic regions, the biofluid is prevented from reaching there and it has access only to the superhydrophilic spots forming a droplet array. Our array gives the user the possibility to gain the same information as working with water-in-oil droplets without the need for external pumping units and with fixed and indexed droplets. We have used this array as a nucleic acid detection platform using SIBA technology and our depicted results showed that this assay is quantitative with a limit of detection down to 1 copy μL^{-1} for 50 µm spot size. In the market leader Bio-Rad ddPCR system, 20 000 droplets are counted using 20 µL PCR-reaction mix. Here, in a chip as small as 2 × 1 cm, we can form 20 000 droplets using reaction mix volume as low as 1 µL.

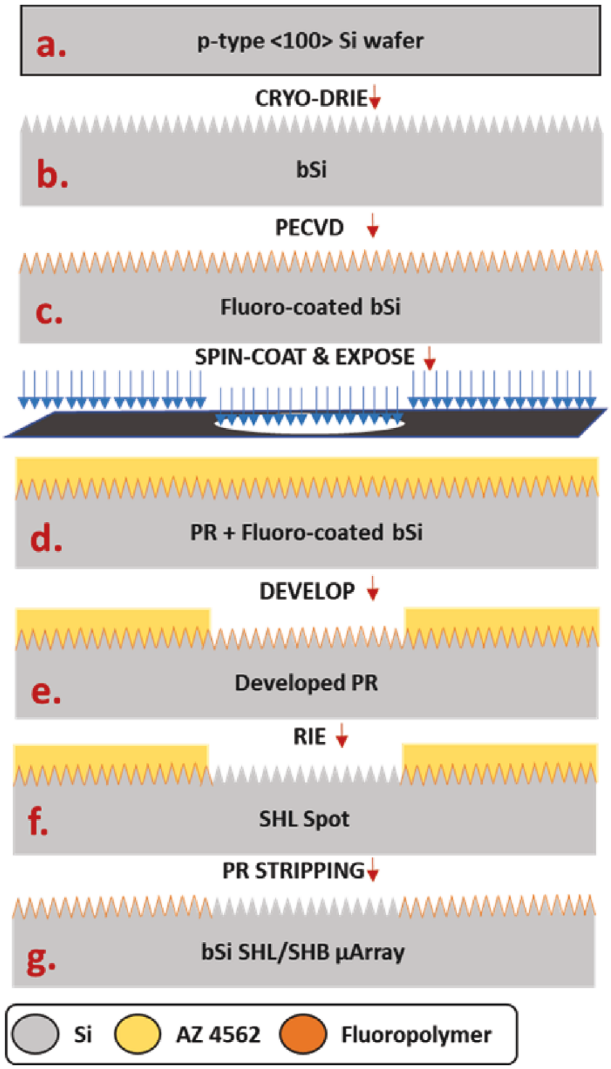

Figure 4. The workflow of patterning the black silicon surface to superhydrophilic/superhydrophobic regions.

4. Experimental Section

Black Silicon Chips Fabrication and Characterization: The SHL/SHB black silicon (bSi) microarray fabrication process is a modified version of the earlier work.[39] **Figure 4** shows the fabrication steps of SHL/SHB patterned bSi. First, bSi was fabricated using a maskless cryogenic deep reactive ion etching (Oxford PlasmaPro 100 Estrelas ICP-DRIE) process on a 4″ silicon wafer (Figure 4a,b). The process parameters were −125 °C temperature, 5 mTorr pressure, ICP power 1500 W, forward power 10 W, and the gas flows were 15 sccm for O_2 and 30 sccm for SF_6. The wafer was then covered with a fluoropolymer hydrophobic coating using a PECVD process (Oxford Plasmalab 80Plus) (Figure 4c). The process parameters were 250 mTorr pressure, 50 W power, and 100 sccm CHF_3 flow. After that, photolithography was performed as follows: AZ 4562 thick photoresist (MicroChemicals) was spin-coated on the bSi surface (4000 rpm for 30 s), soft baked (90 °C, 3 min), exposed for 12 s with different film photomasks (Süss MicroTec MA-6 with 365 nm wavelength), and developed for 10 min in AZ 351B (Merck) to define hydrophilic areas (Figure 4d,e). Next, the fluoropolymer was etched away from the non-protected areas using oxygen plasma reactive ion etching (RIE) (Oxford Plasmalab 80Plus) (Figure 4f). The parameters were 250 mTorr pressure, 50 W power, 45 sccm O_2, and 5 sccm Ar. The photoresist was then removed by ultrasonication in acetone (Figure 4g). The wafer was then diced into small chips with the needed sizes using a dicing saw (DAD3220, Disco). The black silicon structure was confirmed using scanning electron microscopy (SEM). The wetting properties of the surface were characterized using goniometry and fluorescent microscopy.

SU-8 Mold Fabrication: The chamber mold was fabricated using SU-8 photolithography. First, a silicon wafer was dipped in buffered hydrofluoric acid for 5 min. Then, SU-8 100 (Kayaku) was spin-coated on the silicon wafer (1500 rpm, 30 s), and soft baked first at 65 °C for 3 min and then at 95 °C for 5 min (UniTemp GmbH – HP-220). Then, it was exposed for 30 s with a film photomask (Süss MicroTec MA-6 with 365 nm wavelength) and developed for 10 min in MR-DEV 600 (PGMEA) to define the chamber borders. Then, post-exposure baking was performed at 95 °C for 5 min. Finally, a hydrophobic coating was applied using the PECVD process (Oxford Plasmalab 80Plus).

PDMS Casting: Polydimethylsiloxane (PDMS) was prepared by mixing the prepolymer and curing agent at a ratio of 5:1. The degassed mixture was poured over the SU-8 master mold and baked at 65 °C for 3 h to solidify. The PDMS chambers were peeled off the mold and cut to 1 × 1 cm with a height of 200 µm. All chambers were punctured to make an inlet in

the center using a 1.5 mm Miltex Biopsy Punch with Plunder (TED PELLA, Inc).

Water Droplet Microarray: The water droplet microarray was formed by dipping the bSi patterned chip in water and then withdrawing it. After this point, hexadecane oil was used to prevent the droplet's evaporation. The evaporation time of the droplets was measured once in air at room temperature (21 °C) and room relative humidity (40%) and another time under oil at 44 °C using optical microscopy.

Droplet Volume Measurement: Water and SIBA DMA volume on different chips were measured under hexadecane oil using the camera of a contact angle goniometer (THETA, Biolin Scientific). For each chip with a specific SHL spot size and spacing, ten microdroplets from different locations were used to measure static contact angles and baselines. Then, the volume of the droplets was computed using OneAttension software (Biolin Scientific).

Contact Angle and Surface Tension Measurements: Two reference surfaces were used for studying the wettability of a system formed of water, hexadecane, and SIBA. A blank Si wafer exposed to oxygen plasma reactive ion etching (Oxford Plasmalab 80Plus) was used as the hydrophilic (HL) reference surface, and a Si wafer coated with fluoropolymer was used as the hydrophobic (HB) reference surface. The dynamic advancing and receding contact angles were measured using the needle-in-sessile drop technique (THETA, Biolin Scientific). Advancing contact angles were measured from 2 to 5 µL droplet size and receding angles from 5 to 0 µL with a droplet rate of 0.1 µL s^{-1}. The surface tension measurement of SIBA was performed optically using the pendant drop method with a droplet size of 4 µL (THETA, Biolin Scientific). All experiments were performed in triplicates and the reported value is the mean.

SIBA: SIBA SARS-CoV-2 assay from Aidian Oy was performed on the SHL/SHB DMA. The oligos in the assay were designed to amplify the SARS-CoV-2 RNA-dependent RNA-polymerase gene (RdRp). Aidan optimized the SIBA SARS-CoV-2 assay to be used in droplets by creating an optimal fluorescence signal for droplet detection. The assay was SYGRGreen-based.

SIBA Droplet Microarray Formation: All chips, chambers, and equipment used in the RNA detection experiments were sterilized using a UV lamp (365 nm) for 15 min. Figure 2f shows a schematic illustration of SIBA microarray formation. SIBA DMA was formed by first forming a water DMA covered with a thin layer of hexadecane. This was done by immersing the SHL/SHB patterned chip in a water-oil layered system, where the chip was withdrawn from this system starting with the water phase and subsequently passing the oil phase (Figure 2f, **1** and **2**). The excess oil was removed and the PDMS chamber was introduced on the chip. Then, the SIBA mix was flushed in the sealed system using the inlet and the contact time of SIBA mix with the chip was 5 s. The chamber was then disconnected, and the chip was placed in a glass petri dish containing hexadecane (Figure 2f, 3 and 4).

Other Biofluids Used to Validate the Protective Oil Method: The same steps used in the previous subsection (Figure 2f) were repeated using other low-surface tension biofluids to validate the method. First, Evagreen dye (Biotium 20x) was used together with a genomic DNA control in early droplet experiments to demonstrate the fluid exchange in the spots. Evagreen binds to double-stranded DNA and therefore there was no need for an amplification step at this stage. Second, protein-rich cell media was also used to validate the method for droplet microarray formation. The cell media contained high glucose DMEM (Euroclone), 10% FBS (Thermofisher), Penicillin Streptomycin (Gibco), and Glutamax (Gibco) and therefore was high in protein.

dSIBA Experiments: The functionality of the chip was tested using SARS-CoV-2 SIBA from Aidian Oy. SIBA reaction was constructed of SIBA **A** mixture (substrates), SIBA **B** mixture (enzymes), SIBA oligomixture (20 nM oligonucleotides and SYBRGreen), and nuclease-free water. SARS-CoV-2 RNA sample was added to the reaction mixture in a preferable concentration diluted in sample buffer (containing 10 mM magnesium acetate). The total volume of one reaction was 10 µL. The negative control contained only a sample buffer. The reaction was initiated by the addition of magnesium acetate and heating the sample at 44 °C for 20 min. All experiments were performed in triplicates.

Real-Time Detection of SIBA: SIBA reaction was tested together with the hexadecane oil to evaluate whether the oil was interacting with the SIBA reaction. SIBA reaction mixture was prepared as described earlier and loaded into a 384-well plate together with 10 µL of hexadecane oil. RT-qPCR instrument (Bio-Rad) was programmed to keep a constant temperature of 44 °C for 20 min. One cycle was designed to last for 30 s (total of 60 cycles) with a fluorescence readout at the end of each cycle.

Fluorescence Detection and Image Analysis: SIBA assay is based on SYBRGreen chemistry that allows detection via fluorescence microscopy. Pictures were taken using Zeiss Axio imager microscope with 10x magnification and 38HE GFP filter (Biomedicum imaging unit, Helsinki). Tilesfunction was used for imaging large areas (1 × 1 cm). For quantification, ImageJ was employed by counting 10 000 droplets using an automated particle counter. The software first converted the picture to black and white and the fluorescence background was determined based on signal intensity in the negative control and used for determining positive and negative spots. Then, size and circularity filters were applied to exclude any defects. AI was also used by implementing Aiforia Create Version 5.5 (Aiforia Technologies Plc, Helsinki, Finland), and the results were compared to ImageJ analysis. The deep convolutional neural network was taught to recognize positive, negative, and empty spots from the fluorescence pictures (see Figure S6, Supporting Information) Aiforia showed a total object error of 0.25% (consisting of false positive 0.16% and false negative 0.08% errors) between all of the analyzed pictures.

Supporting Information

Supporting Information is available from the Wiley Online Library or from the author.

Acknowledgements

This work utilized the cleanroom facilities of Micronova, which is part of the OtaNano national research infrastructure. Imaging was done at the Biomedicum Imaging Unit, Helsinki University, Finland, with the support of Biocenter Finland. This work was funded by the Academy of Finland (#341459). P.E. would also like to acknowledge the Doctoral Programme in Clinical Research for her studentship.

Conflict of Interest

All SIBA patents/patent applications are owned by Aidian Oy. T.O. is an employee of Aidian Oy.

Author Contributions

M.A. and P.E. contributed equally to this work. M.A., P.E., and V.J. proposed and designed the research. M.A. did the surface fabrication and characterization, performed the wettability studies, and analyzed the data. P.E. developed and validated SIBA reaction in droplets. M.A. and P.E. performed the nucleic acid detection experiments on the patterned surface, did fluorescence microscopy, and analyzed the data. T.O. provided SIBA mixture. P.S. provided valuable advice for digital nucleic acid detection. V.J. developed the concept of using protective oil coating for the formation of droplet microarray of low surface tension biofluids. M.A. and P.E. wrote the paper. V.J. carried out the review and editing. T.O. and P.S. reviewed the article.

Data Availability Statement

The data that support the findings of this study are available from the corresponding author upon reasonable request.

Keywords

biofluids, black silicon, digital nucleic acid amplification, microfluidics, wettability patterning

Received: July 12, 2023
Revised: August 20, 2023
Published online: October 23, 2023

[1] W. Feng, E. Ueda, P. A. Levkin, *Adv. Mater.* **2018**, *30*, 1706111.
[2] Y. Zhu, Y.-X. Zhang, W.-W. Liu, Y. Ma, Q. Fang, B.o Yao, *Sci. Rep.* **2015**, *5*, 9551.
[3] W.-W. Liu, Y. Zhu, Y.i-M. Feng, J. Fang, Q. Fang, *Anal. Chem.* **2017**, *89*, 822.
[4] Y. Sun, X. Zhou, Y. Yu, *Lab Chip* **2014**, *14*, 3603.
[5] Z. Dong, Q. Fang, *Trends Analyt. Chem.* **2020**, *124*, 115812.
[6] A. A. Popova, K. Demir, T. G. Hartanto, E. Schmitt, P. A. Levkin, *RSC Adv.* **2016**, *6*, 38263.
[7] A. A. Popova, S. M. Schillo, K. Demir, E. Ueda, A. Nesterov-Mueller, P. A. Levkin, *Adv. Mater.* **2015**, *27*, 5217.
[8] P. Raittinen, P. Elomaa, P. Saavalainen, V. Jokinen, *Adv. Mater. Interfaces* **2021**, *8*, 2100147.
[9] O. Vandenberg, D. Martiny, O. Rochas, A. Van Belkum, Z. Kozlakidis, *Nat. Rev. Microbiol.* **2021**, *19*, 171.
[10] L. Benevides Lima, F. P. Mesquita, L. L. Brasil De Oliveira, F. Andréa Da Silva Oliveira, M. Elisabete Amaral De Moraes, P. F. N. Souza, R. C. Montenegro, *Expert Rev. Mol. Diagn.* **2022**, *22*, 157.
[11] L. Dong, J. Zhou, C. Niu, Q. Wang, Y. Pan, S. Sheng, X. Wang, Y. Zhang, J. Yang, M. Liu, Y. Zhao, X. Zhang, T. Zhu, T. Peng, J. Xie, Y. Gao, D.i Wang, X. Dai, X. Fang, *Talanta* **2021**, *224*, 121726.
[12] L.i-P. Xu, Y. Chen, G. Yang, W. Shi, B. Dai, G. Li, Y. Cao, Y. Wen, X. Zhang, S. Wang, *Adv. Mater.* **2015**, *27*, 6878.
[13] M. Baker, *Nat. Methods* **2012**, *9*, 541.
[14] A. S. Whale, J. F. Huggett, S. Cowen, V. Speirs, J. Shaw, S. Ellison, C. A. Foy, D. J. Scott, *Nucleic Acids Res.* **2012**, e82, *40*.
[15] L. Zanoli, G. Spoto, *Biosensors* **2012**, *3*, 18.
[16] L. Chen, V. Yadav, C. Zhang, X. Huo, C. Wang, S. Senapati, H.-C. Chang, *Anal. Chem.* **2021**, *93*, 6456.
[17] K. A. Heyries, C. Tropini, M. Vaninsberghe, C. Doolin, O. I. Petriv, A. Singhal, K. Leung, C. B. Hughesman, C. L. Hansen, *Nat. Methods* **2011**, *8*, 649.
[18] Y. Men, Y. Fu, Z. Chen, P. A. Sims, W. J. Greenleaf, Y. Huang, *Anal. Chem.* **2012**, *84*, 4262.
[19] L. Cao, X. Guo, P. Mao, Y. Ren, Z. Li, M. You, J. Hu, M. Tian, C. Yao, F. Li, F. Xu, *ACS Sens.* **2021**, *6*, 3564.
[20] Q. Zhu, Y. Xu, L. Qiu, C. Ma, B. Yu, Q.i Song, W. Jin, Q. Jin, J. Liu, Y. Mu, *Lab Chip* **2017**, *17*, 1655.
[21] C. D. Ahrberg, J. M. Lee, B. G. Chung, *BioChip J.* **2019**, *13*, 269.
[22] Y. Seo, S. Jeong, J. Lee, H. S. Choi, J. Kim, H. Lee, *Nano Converg.* **2018**, *5*, 9.
[23] C. D. Ahrberg, J.i W. Choi, J. M. Lee, K. G. Lee, S. J. Lee, A. Manz, B. G. Chung, *Lab Chip* **2020**, *20*, 3560.
[24] S. Bhat, J. Herrmann, P. Armishaw, P. Corbisier, K. R. Emslie, *Anal. Bioanal. Chem.* **2009**, *394*, 457.
[25] L. Du, Y. Li, X. Zhang, Z. Zhou, Y. Wang, D. Jing, J. Zhou, *ACS Appl. Mater. Interfaces* **2023**, *15*, 17413.
[26] M. J. Hoser, H. K. Mansukoski, S. W. Morrical, K. E. Eboigbodin, *PLoS One* **2014**, *9*, e112656.
[27] K. E. Eboigbodin, K. Moilanen, S. Elf, M. Hoser, *BMC Infect. Dis.* **2017**, *17*, 134.
[28] K. Xu, X. Wang, R. M. Ford, J. P. Landers, *Anal. Chem.* **2016**, *88*, 2652.
[29] N. K. Mandsberg, O. Hansen, R. Taboryski, *Sci. Rep.* **2017**, *7*, 12794.
[30] B.o Chang, Q. Zhou, R. H. A. Ras, A. Shah, Z. Wu, K. Hjort, *Appl. Phys. Lett.* **2016**, *108*, 154102.
[31] N. Ramalingam, M. E. Warkiani, N. Ramalingam, G. Keshavarzi, L. Hao-Bing, T. G. Hai-Qing, *Biomed. Microdevices* **2016**, *18*, 68.
[32] S. Qian, H. Wu, B. Huang, Q.i Liu, Y. Chen, B.o Zheng, *Sens Actuators B Chem* **2021**, *345*, 130341.
[33] Y. Sun, in *Nucleic Acid Amplification Strategies for Biosensing, Bioimaging and Biomedicine* (Eds.: S. Zhang, S. Bi, X. Song), Springer, Berlin, Germany **2019**.
[34] A. Peethan, M. Aravind, V. K. Unnikrishnan, S. Chidangil, S. D. George, *Appl. Surf. Sci.* **2022**, 151188, *571*.
[35] Y. Wang, B. Zhang, H. Dodiuk, S. Kenig, C. Barry, J. Ratto, J. Mead, Z. Jia, S. Turkoglu, J. Zhang, *ACS Appl. Mater. Interfaces* **2021**, *13*, 58096.
[36] Y. Xia, S. Yan, X. Zhang, P. Ma, W. Du, X. Feng, B.i-F. Liu, *Anal. Chem.* **2017**, *89*, 3716.
[37] J. Chi, C. Shao, X. Du, H. Liu, Z. Gu, *ACS Appl. Mater. Interfaces* **2018**, *10*, 39144.
[38] P. Mao, L. Cao, Z. Li, M. You, B. Gao, X. Xie, Z. Xue, P. Peng, C. Yao, F. Xu, *Analyst* **2021**, *146*, 6960.
[39] V. Jokinen, L. Sainiemi, S. Franssila, *Adv. Mater.* **2008**, *20*, 3453.